THE JOURNAL OF BIOLOGICAL CHEMISTRY VOL. 287, NO. 14, pp. 11437–11445, March 30, 2012
Published in the U.S.A.

Affixing N-terminal α-Helix to the Wall of the Voltage-dependent Anion Channel Does Not Prevent Its Voltage Gating*[S]

Received for publication, October 15, 2011, and in revised form, January 10, 2012 Published, JBC Papers in Press, January 24, 2012, DOI 10.1074/jbc.M111.314229

Oscar Teijido[‡1], Rachna Ujwal[§1], Carl-Olof Hillerdal[¶], Lisen Kullman[¶], Tatiana K. Rostovtseva[‡2], and Jeff Abramson[§3]

From the [‡]Program in Physical Biology, Eunice Kennedy Shriver NICHD, National Institutes of Health, Bethesda, Maryland 20892, the [§]Department of Physiology at the David Geffen School of Medicine, UCLA, Los Angeles, California 90095, and the [¶]Department of Medical Cell Biology, Uppsala University, 751 23 Uppsala, Sweden

Background: There is ongoing controversy concerning the location and mobility of the N-terminal α-helix in VDAC1 during voltage gating.
Results: mVDAC1 with the N-terminal α-helix cross-linked to β-strand 11 forms typical voltage-gated channels.
Conclusion: The N-terminal domain of VDAC1 does not move independently during voltage gating.
Significance: This study dramatically alters the current view of voltage gating dynamic in VDAC1.

The voltage-dependent anion channel (VDAC) governs the free exchange of ions and metabolites between the mitochondria and the rest of the cell. The three-dimensional structure of VDAC1 reveals a channel formed by 19 β-strands and an N-terminal α-helix located near the midpoint of the pore. The position of this α-helix causes a narrowing of the cavity, but ample space for metabolite passage remains. The participation of the N-terminus of VDAC1 in the voltage-gating process has been well established, but the molecular mechanism continues to be debated; however, the majority of models entail large conformational changes of this N-terminal segment. Here we report that the pore-lining N-terminal α-helix *does not* undergo independent structural rearrangements during channel gating. We engineered a double Cys mutant in murine VDAC1 that cross-links the α-helix to the wall of the β-barrel pore and reconstituted the modified protein into planar lipid bilayers. The modified murine VDAC1 exhibited typical voltage gating. These results suggest that the N-terminal α-helix is located inside the pore of VDAC in the open state and remains associated with β-strand 11 of the pore wall during voltage gating.

The voltage-dependent anion channel (VDAC)[4] serves as the primary conduit between the mitochondria and the rest of the cell, facilitating free exchange of ions and metabolites across the outer mitochondrial membrane. In addition to its metabolic and energetic functions, VDAC has a more complex role, serving as a receptor for molecules and proteins that modulate the organelle's permeability and thereby its function (1–3). This multifunctional channel has been implicated in the metabolic stresses of cancer, cardiovascular disease, and mitochondrial-dependent cell death (4–8); thus, understanding the structure and function of VDAC constitutes a critical objective for basic as well as medical research.

Single channel conductance experiments on VDAC1 at low membrane potential (<30 mV) reveal a high conductance (4.1 ± 0.1 nanosiemens in 1 M KCl) indicative of a large pore, usually referred to as the "open" state of the channel (1). This conformer facilitates the passage of 10^6 ATP molecules (9) and displays a preference for monovalent anions over cations with the anion-to-cation permeability ratio of 2:1 in high salt (10) and 4:1 in physiological salt concentration (11). As voltage is increased (>30 mV) in either a positive or a negative direction, the channel switches into the lower conducting states (around 2 nanosiemens in 1 M KCl), termed as the "closed" state(s). These states are cation-selective with a negligible metabolite flux (9, 12). The transitions between the open and the closed states involve large conformational changes (13, 14) constituting a gating action that both hinders the passage of metabolites and alters ion selectivity (1). Colombini and co-workers (1, 14–16) performed extensive electrophysiological and biochemical analyses of VDAC properties using site-directed mutagenesis and biotin modification studies. Based on these data, they developed a model for VDAC voltage gating where the N-terminal segment is an essential component of the mobile voltage sensor domain, which slides in and out of the channel lumen in response to the applied voltage (1, 14, 15). Several additional studies have reported alternative models in which the N-terminal segment is exposed to the cytoplasm (7, 17, 18) or resides on the membrane surface (19, 20). Although the proposed mechanism of voltage gating differs among investigators, most models involve large conformational changes of the N-terminal segment.

In 2008, three groups reported, with increasing atomic detail, the long sought after structure of VDAC1 (21–23). All three structures showed a large pore composed of 19 β-strands with

* This work was supported, in whole or in part, by the Intramural Research Program of the Eunice Kennedy Shriver NICHD, National Institutes of Health (to O. T. and T. K. R.) and National Institutes of Health Grant RO1 GM078844 (to J. A.).
[S] This article contains supplemental Fig. 1 and Table 1.
[1] Both authors contributed equally to this work.
[2] To whom correspondence may be addressed. E-mail: rostovtt@mail.nih.gov.
[3] To whom correspondence may be addressed: E-mail: jabramson@mednet.ucla.edu.
[4] The abbreviations used are: VDAC, voltage-dependent anion channel; Cu-Ph, $CuSO_4$-phenanthroline; TMRM, tetramethylrhodamine 5-maleimide; mVDAC1, murine VDAC1.

the high resolution structure of murine VDAC1 (mVDAC1) revealing the precise orientation of the N-terminal voltage-sensing domain (Fig. 1). The α-helical portion of the N-terminal segment is positioned halfway through the pore, causing a narrowing of the cavity, where it is ideally situated to regulate metabolite flux. Thus, it was believed that the transition between conformations required a repositioning of the N-terminal segment. Here we report that, unexpectedly, the N-terminal segment of VDAC1, which lines the channel pore, *does not* undergo independent dynamic structural rearrangements during channel gating. We show that cross-linking of the α-helical portion of the N-terminal segment to the wall of the pore does not prevent VDAC1 voltage gating when inserted in planar lipid bilayers. These results suggest that the N-terminal α-helix is located inside the pore when VDAC1 is open and remains stably associated with residue 170 of the β-barrel wall during voltage gating.

MATERIALS AND METHODS

Cloning, Recombinant Protein Production, and Purification—All mutants were engineered using Stratagene's QuikChange site-directed mutagenesis kit (La Jolla, CA). A Cys-less mVDAC1 construct (CL-mVDAC1) was generated by mutating Cys-127 and Cys-232 to alanines. Using the CL-mVDAC1 construct, cysteine residues were engineered at position 10 (L10C) and position 170 (A170C) to generate a double cysteine mutant (VDAC-Cys).

Recombinant protein expression and purification were carried out as described previously (23). Briefly, a two-step purification procedure consisting of Talon affinity and size exclusion chromatography was performed to isolate a homogenous population of murine His-tagged VDAC1 WT and VDAC-Cys. Purified protein was washed using an Amicon 30-kDa cut-off concentrator to replace the size exclusion chromatography buffer with 20 mM Tris, pH 8.0, 50 mM NaCl, 0.1% LDAO. Aggregated protein was removed by ultracentrifugation at 430,000 $\times$ *g* for 30 min, and the concentration was determined using absorption at 280 nm.

Cross-linking—Cysteine mutants described above (VDAC-Cys) were used to cross-link the mVDAC1 N-terminal region to the β-barrel using a mix of copper/phenanthroline as a cross-linking reagent. The metal chelator α-phenanthroline, in combination with trace amounts of cupric ion, catalyzed the oxidation of the sulfhydryl groups of cysteines to form disulfide bonds (24). This reaction could be reversed by reducing agents, such as DTT. The cross-linking reaction was performed by using a copper and α-phenanthroline mix ($CuSO_4$-phenanthroline; Cu-Ph). Briefly, 0.005 g of $CuSO_4$ was dissolved in 75 μl of double-distilled water, and 0.012 g of phenanthroline was dissolved in 25 μl of 100% ethanol and 25 μl of double-distilled water. Both solutions were then mixed stepwise (*i.e.* 25-μl aliquots of $CuSO_4$ were added to the phenanthroline solution and mixed by vortex) in order to avoid the formation of precipitates. Serial dilutions were then prepared from the stock solution of 150 mM Cu-Ph.

Cross-linking reactions, "in tube," were performed by mixing 20 μl of 0.1 mg/ml VDAC-Cys with 0.02 mM Cu-Ph followed by incubation for 10 min at room temperature. The rest of the experiment was performed on ice. Cross-linking was reversed by the addition of 100 μM DTT to the VDAC-Cys or to the VDAC-Cys with 0.02 mM Cu-Ph mix. To monitor the cross-linking efficiency, cross-linked samples were analyzed on SDS-PAGE after tetramethylrhodamine 5-maleimide (TMRM) labeling (described below).

TMRM Labeling—TMRM (Sigma) was dissolved in 100% DMSO. Purified mVDAC1 was incubated with a 10-fold molar excess of TMRM for 15 min at room temperature. The reaction was stopped by the addition of SDS-PAGE loading buffer. 10 μg of protein samples were run on a 12% SDS-PAGE. Detection of TMRM was carried out using UV light (Gene Flash Syngene Bio Imaging). Gels were subsequently stained with R-250 Coomassie Brilliant Blue to visualize loading quantities.

VDAC Reconstitution and Conductance Measurements—Planar lipid membranes were formed on a 70–90 μm diameter orifice in a 15-μm-thick Teflon partition that separated two chambers as described previously (25). Lipid monolayers used for membrane formation were made from a 5 mg/ml solution of diphytanoylphosphatidylcholine (Avanti Polar Lipids, Inc.) in pentane. Channel insertion was achieved by adding 0.3 $\pm$ 0.1 μl of mVDAC1 WT (stock: 0.01 mg/ml in LDAO buffer) or 1.5 $\pm$ 0.8 μl of VDAC-Cys (stock: 0.1 mg/ml in LDAO buffer) into the 1.2-ml aqueous phase of the *cis* compartment while stirring. Aqueous solutions of 1 M KCl were buffered with 5 mM HEPES at pH 7.4. Potential was defined as positive when it was greater at the side of the VDAC addition (*cis*-side). Current recordings were performed as described previously (25) using an Axopatch 200B amplifier (Axon Instruments, Inc., Foster City, CA) in the voltage-clamp mode. Single-channel data were filtered by a low pass 8-pole Butterworth filter (model LPF-8, Warner Instrument Corp.) at 15 kHz and directly saved with a sampling frequency of 50 kHz.

The voltage-dependent properties of a VDAC-containing membrane were assessed following the protocol devised by Colombini and co-workers (10, 26) in which gating is inferred from the channel response to slowly changing periodic voltage waves applied. A symmetrical 5 mHz triangular voltage wave with $\pm$60 mV amplitude from a Function Waveform Generator 33120A (Hewlett Packard) was used. Data were acquired with a Digidata 1322A board (Axon Instruments Inc.) at a sampling frequency of 1Hz and analyzed using the pClamp 10.2 software (Axon Instruments, Inc.). Analysis of VDAC voltage gating was performed following Ref. 10 and as described in Ref. 25. Two gating parameters (*n*, which is the effective gating charge and is the measure of the voltage-dependence steepness, and V_0, the voltage at which half of the channels are open and half are closed) were calculated from the open probability plots following Ref. 10 as described previously (25). Plot fitting was performed through the logarithmic version of the Boltzman distribution equation (25).

After VDAC-Cys was incubated with different concentrations of Cu-Ph in tube, the cross-linked VDAC was then reconstituted into the planar lipid bilayers as described above. Cross-linking reactions were reversed by the addition of 100 μM DTT to VDAC-Cys in tube before channel reconstitution into the membrane or by the addition of 100 μM DTT "in bath," after membrane reconstitution of VDAC-Cys. Cross-linking reactions in bath were performed on VDAC-Cys already reconsti-

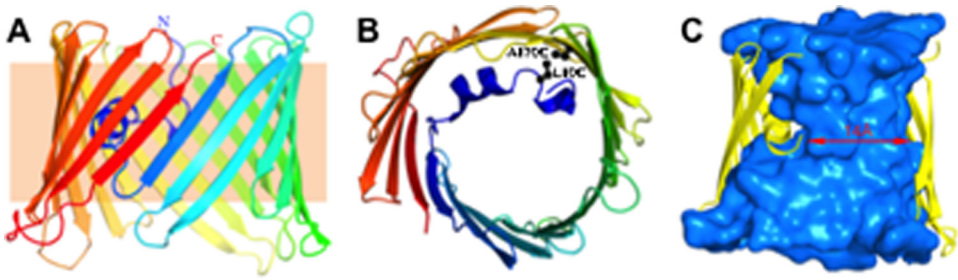

FIGURE 1. **Overall structure of VDAC1.** *A*, schematic representation of VDAC1 viewed parallel to the plane of the membrane. The protein is *colored* from the N terminus in *blue* to the C terminus in *red*. *B*, schematic representation of mVDAC1 viewed perpendicular to the membrane plane. Positions of Leu-10 and Ala-170 are displayed in *ball and stick form*. *C*, same view as in *A* with β-strands 19 and 1–4 removed. The interior surface of the VDAC1 channel (*cyan*), created using the program HOLLOW (48), illustrates the contour of the pore. Dimensions along the narrowest point in the center of the pore are displayed.

tuted into planar membrane. When single or multiple channels were incorporated into the membrane and their conductance and voltage gating properties were established, Cu-Ph was added directly to the membrane-surrounding aqueous solutions to both sides of the membrane under constant stirring, and channel properties were monitored 10 min after the Cu-Ph addition.

RESULTS

Cross-linking of α-Helical Portion of N-terminal Segment to β-Strand 11—Previously, we resolved the structure of mVDAC1 at 2.3 Å resolution using the technique of lipidic bicelle crystallization (27, 28). The structures of mVDAC1 reveal a unique 19-strand β-barrel (Fig. 1*A*) arranged in an antiparallel pattern with the exception of strands β1 and β19, which associate in a parallel manner to seal the barrel. The exterior of the β-barrel primarily consists of hydrophobic residues that are exposed to the lipid environment, whereas the interior is extensively hydrophilic, making it conducive for the passage of ions and large metabolites through the outer mitochondrial membrane. From both sides of the membrane, the channel's opening resembles an hourglass with a maximal inner dimension of 27 × 24 Å. Approximately halfway through the pore, the N-terminal α-helix segment (aligned nearly parallel to the plane of the membrane) causes a partial narrowing of the cavity to 27 × 14 Å (Fig. 1*C*), yet ample space remains for the passage of metabolites in this arrangement. Thus, this structure probably represents the open conformation, a claim substantiated by our recent computations (29). Numerous studies have established the importance of the N-terminal α-helix in regulating the flux of ions and metabolites through the channel, and the observation that it is localized within the pore (21–23) makes it ideally suited to regulate their passage. Furthermore, the N-terminal region is widely believed to be flexible with a potential for large structural rearrangements, in response to stimuli that alter the channel's properties (7, 16–18, 20, 23, 30–32).

Closer examination of the mVDAC1 structure shows that the N-terminal segment (amino acids 1–26) has extensive hydrophobic interactions and hydrogen bonds with the interior wall of the pore (adjacent to β-strands 8–19), facilitating its orientation (Fig. 1*B*). In the current structure, Leu-10 (located on the N-terminal α-helix) and Ala-170 (located on the β-strand 11) are ideally positioned to form a disulfide bond (Fig. 1*B*), which would "lock" the α-helix to the pore wall. To accomplish this, an initial Cys-less mVDAC1 construct (CL-mVDAC1) was generated by mutating the two endogenous cysteine residues to alanines (C127A and C232A). In this Cys-less background (CL), cysteines at position 10 (L10C-CL) and at position 170 (A170C-CL) were introduced, and their accessibility was monitored using the fluorescent chromophore TMRM, which forms a covalent bond with accessible Cys residues. This reaction is easily monitored in gels by following the fluorescence of TMRM (33). Fig. 2*B* (*left*) shows that TMRM fluorescence is eliminated in the CL background (*lane 2*). When Cys was engineered at position 170 or 10 (*lanes 3* and *4*, respectively), the TMRM fluorescence was reestablished. The cysteine accessibility was also monitored in the double cysteine mutant L10C/A170C (VDAC-Cys) (Fig. 2*B*, *right*), which still retained its proper function (Figs. 3*B*, 4*B*, and 5).

A cross-link was generated between positions 10 and 170 by incubating the sample with 0.02 mM Cu-Ph, an oxidizing agent that induces disulfide formation. After the addition of the Cu-Ph, the accessibility was again tested, and *no* fluorescence was observed, indicative of a disulfide bond involving the two cysteine residues (Fig. 2*B*, *right*). In addition, after cross-linking, a large gel shift was observed, resulting in the L10C/A170C cross-linked sample running lower on the gel (Fig. 2). This gel shift was reversible upon the addition of the reducing agent DTT (Fig. 2*A*), and TMRM accessibility was restored. Similar features have been observed in other outer membrane proteins that exhibited cross-linking (34, 35).

Characterization of L10C/A170C Double Cysteine Mutant in Planar Lipid Bilayers—A representative current record of the VDAC1 WT reconstituted into planar lipid bilayer is shown in Fig. 3*A* (VDAC WT). Increasing applied voltage, in either the positive or negative direction, resulted in the characteristic VDAC voltage gating where the channel switches from a high conducting state referred to as the "open" conformation, which facilitates the passage of ATP and other nucleotides, to the variety of the lower conducting or "closed" states that are essentially impermeable to ATP. Similarly, the L10C/A170C mutant protein in the Cys-less background (VDAC-Cys) showed the characteristic VDAC voltage gating as it transitioned between open and multiple closed states (Fig. 3*B*). Cross-linking was initiated by the addition of 0.02, 0.2, and 0.8 mM Cu-Ph to the membrane-surrounding buffer. All cross-linked proteins, even at the highest concentration of Cu-Ph, also formed normal fully functioning channels in planar membranes (Fig. 3, *C–E*). These

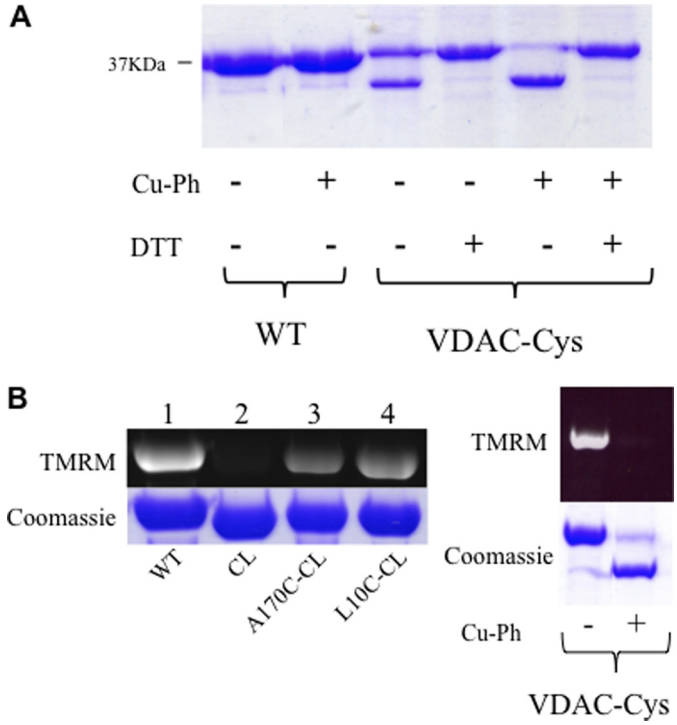

FIGURE 2. **Cross-linking of the N-terminal region with the β-barrel.** *A*, Coomassie-stained gel of wild type (*WT*) and double Cys mutant L10C/A170C (*VDAC-Cys*). The protein was incubated in the presence (+) and absence (−) of Cu-Ph (5:1 molar ratio) and 10 mM DTT. The lower band is indicative of disulfide bond formation. *B*, TMRM labeling of Cys residues. Purified VDAC was incubated with a 10-fold molar excess of TMRM for 15 min at room temperature. The reaction was stopped by the addition of SDS-PAGE loading buffer. 10 μg protein samples were run on a 12% SDS-polyacrylamide gel. Detection of TMRM was carried out using UV light. Cys-less (*CL*) and cross-linked samples (*VDAC-Cys Cu-Ph* +) displayed no fluorescence because no Cys residues were available to react with TMRM.

results strongly indicate that the N-terminal segment does not undergo independent conformational changes during voltage gating.

To establish that the gating behavior recorded was representative for the majority of mVDAC1 channels undergoing this transition, we repeated these experiments using multichannel recordings on membranes with an average of 20 channels reconstituted at once (Fig. 4). Again, the WT and the L10C/A170C mutant proteins with and without Cu-Ph (0.6 and 1.3 mM) in the membrane-bathing solutions consistently behaved analogously. Analysis of the probability of VDAC to be open or closed at varying potentials (Fig. 5*A*) showed similar voltage gating for VDAC-Cys regardless of the presence of cross-linker in the bathing solution, once again indicating that the cross-linking does not inhibit or reduce voltage gating as one would anticipate if the N-terminal segment undergoes independent large conformational changes. Furthermore, the VDAC-Cys showed higher voltage sensitivity at positive potentials, as observed by a shift in the open probability curves to the lower potentials (Fig. 5*A* and Table 1).

It is possible that once inserted into the bilayer, the VDAC-Cys assumes a different conformation (36), which is not permissive for disulfide formation. To ensure that a proper cross-link was formed between the β-strand and the α-helix, the sample was preincubated with 0.02, 0.8, and 10 mM Cu-Ph prior to reconstitution into the planar membranes (Fig. 5*B*). This reaction was monitored by TMRM labeling (Fig. 2*B*). Once again, these cross-linked samples maintained typical VDAC voltage gating in planar membranes and shifted the open probability to the lower potentials with respect to the WT protein (Fig. 5*B* and Table 1). Alternatively, the VDAC-Cys was treated with 0.1 mM DTT, in order to reduce the disulfide bond, prior to protein reconstitution into the membrane. Interestingly, the open probability curve and voltage-gating parameters obtained under these conditions were nearly identical to those of the VDAC WT (Fig. 5*B* and Table 1). The same effect was observed when 0.1 mM DTT was added directly to the membrane-surrounding buffer solution after VDAC-Cys (pretreated with 0.02 mM Cu-Ph in tube) was reconstituted into the membrane (supplemental Fig. 1 and Table 1). In conclusion, cross-linked VDAC forms functional channels in planar lipid membranes with typical conductance and voltage gating. These new data indicate that the N-terminal domain *does not* move independently during voltage gating, resulting in large structural rearrangements, as suggested by several previous studies (7, 17, 18, 20, 23, 32). The N terminus remains affixed to β-strand 11 of the pore wall, or if in motion, it moves in coordinated motion with the rest of the voltage sensor domain.

DISCUSSION

There is considerable evidence demonstrating that VDAC undergoes large conformational changes during voltage-dependent gating (1, 13, 14), and many studies have attributed these changes to movements of the N-terminal segment (7, 17, 18, 20, 23, 32, 37). By a combination of site-directed mutagenesis, induced disulfide bond formation, and electrophysiological characterization in planar lipid bilayers, we have shown that VDAC with the N-terminal α-helix portion engineered to covalently bind the pore wall behaves indistinguishably from endogenous protein, suggesting that the N-terminal segment is either not mobile or does not move independently of the rest of the voltage-sensor domain during gating.

In addition to changes in membrane potential, different factors shift the dynamic equilibrium of VDAC toward the closed conformation, including protein-protein interactions (2, 38–41), low pH (10, 42), or the binding of NADH (10). To date, there are a number of proposed mechanisms for achieving gating through the N-terminal segment (23, 30, 43). In our initial report of the mVDAC1 structure, the stimuli mentioned above were believed to disrupt the interactions between the N-terminal helix and the β-barrel wall, resulting in a reorientation within the channel lumen to adopt the more occlusive conformation of the pore (23). Further evidence in support of alterations in the position of the α-helix came from the NMR structure of human VDAC1 (21), which showed an NADH interaction site on β-strands 17 and 18. The position of the NADH site flanks a flexible region (Gly-21, Tyr-22, Gly-23, Phe-24, and Gly-25) of the N-terminal segment, and the mVDAC1 structure clearly demonstrates that there is insufficient space for NADH binding in this region. Thus, the N-terminal segment would have to be repositioned to accommodate NADH.

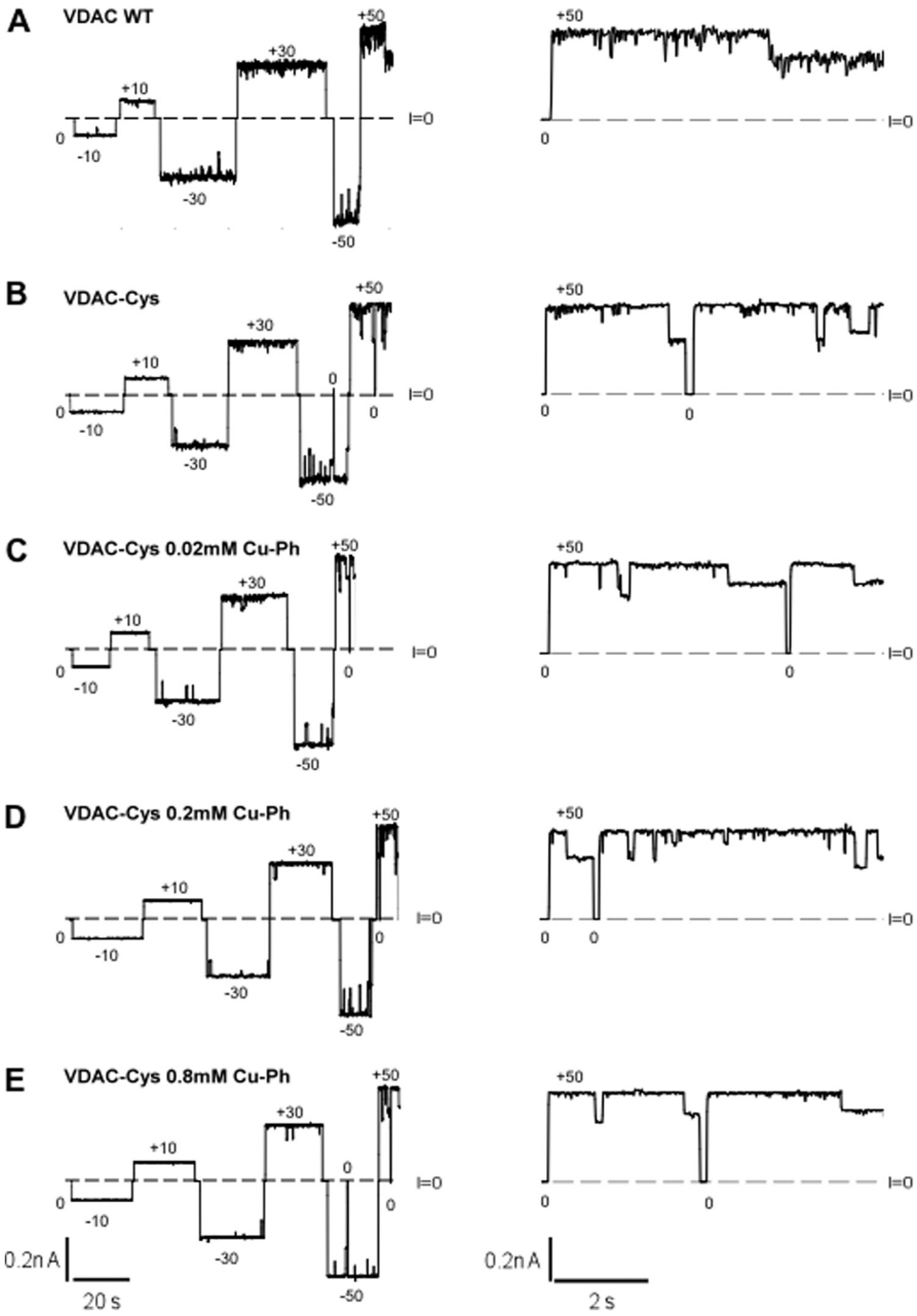

FIGURE 3. **Cross-linking of the N-terminal region with the β-barrel does not change the electrophysiological properties of VDAC.** Shown are representative records of ion currents through two channels formed by VDAC WT (*A*); VDAC-Cys (*B*); and VDAC-Cys treated with 0.02 (*C*), 0.2 (*D*), or 0.8 mM (*E*) cross-linker Cu-Ph, respectively. After channels were reconstituted into the planar bilayer, increasing concentrations of Cu-Ph (*C–E*) were added into the membrane-surrounding buffer solutions consisting of 1 M KCl and 5 mM HEPES at pH 7.4. Cu-Ph was added to both sides of the membrane. *Dashed lines*, zero current levels. Applied voltages in mV are indicated. Traces in fine time scale at +50 mV of applied voltage are shown on the *right*. Characteristic VDAC voltage gating is observed as transitions between one high conducting open and multiple low conducting closed states for the WT and the cross-linked VDAC. Current records were digitally filtered with a Bessel low-pass filter at 100 Hz.

Colombini and colleagues (16, 36) have previously generated a topology model of VDAC, derived from biochemical and electrophysiological assays, where 13 β-strands and a single α-helix form the pore of the channel. In this model, the voltage-sensitive domain of VDAC is mobile and forms a large portion of the pore wall, including the N-terminal segment. They further asserted that upon application of voltage, large conformational changes would be required for changing the pore's dimension, conductance, and reversal of ion selectivity. However, according to this two-dimensional topology, the N-terminal α-helix is part of the pore's wall (including position Leu-10), and Ala-170 is located in a loop in the presumably intermembrane space between β-strands 8 and 9 (according to the numbering in Refs. 16 and 36). If

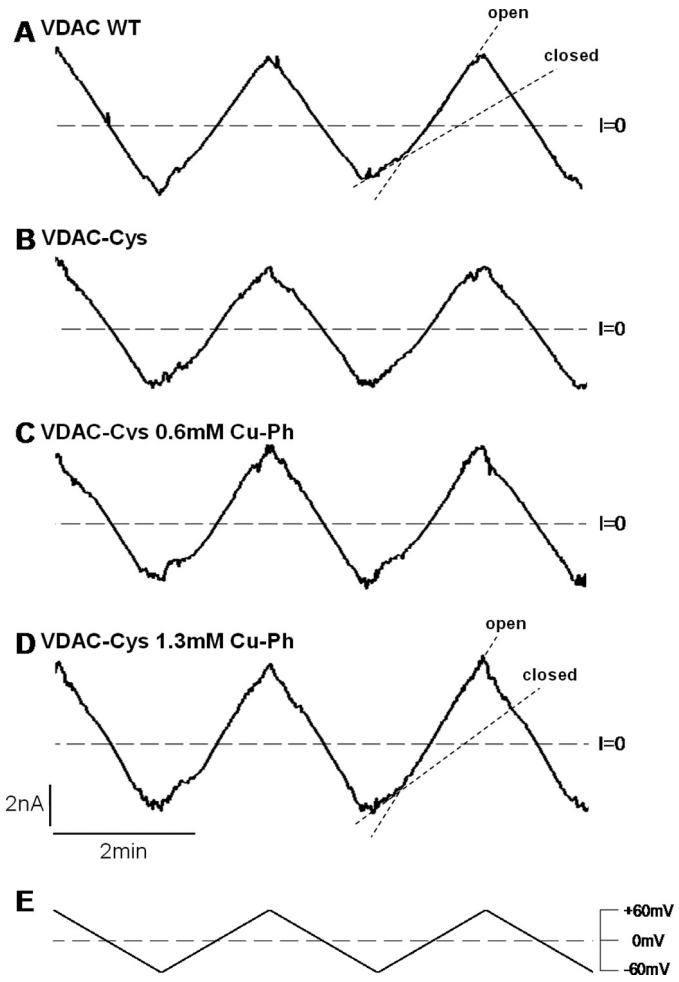

FIGURE 4. **Cross-linking does not inhibit VDAC-Cys voltage gating.** Traces of ion currents through multichannel membranes with reconstituted VDAC WT (*A*), VDAC-Cys (*B*), and VDAC-Cys treated with 0.6 or 1.3 mM cross-linker Cu-Ph (*C* and *D*). After the insertion of an average of 20 channels into the planar membrane, Cu-Ph was added into the membrane-surrounding buffer solutions consisting of 1 M KCl solution (pH 7.4). Traces in *A–D* correspond to current responses to the continuously changing triangular voltage waves (5 mHz, ±60 mV) shown in *E*. Steep slopes at low potentials correspond to the high conductance of open channels, whereas the irregular low slopes at higher potentials correspond to the low conductance of closed states (*dotted lines* in *A* and *D*). *Dashed lines*, zero current levels.

this were the case, residues Leu-10 and Ala-170 would be too far to form a disulfide bond.

It should be noted that only a small population of protein is inserted into the bilayer, and, although unlikely, there remains the possibility that the protein measured in bilayers has not been cross-linked. We have attempted to address this issue by demonstrating nearly complete cross-linking (Fig. 2) before channel reconstitution into the bilayer and performing multiple measurements (a minimum of three replicates) on membranes reconstituted with multiple channels (~20 channels) (Figs. 4 and 5). Furthermore, only the L10C/A170C mutant, before or after the cross-linker addition, shows a lower open probability at positive potentials than VDAC WT (Fig. 5 and Table 1), demonstrating that there is a quantitative difference in gating parameters between wild type and cross-linked protein. Indeed, V_0, the characteristic voltage at which half-channels are open, is ~20 mV lower for the cross-linked VDAC-Cys (16–19 mV) than for VDAC WT (37 ± 2 mV) (Table 1). The V_0 value of non-cross-linked VDAC-Cys lies between those of WT and cross-linked protein (25 mV), suggesting that part of VDAC-Cys was spontaneously cross-linked without Cu-Ph treatment. Importantly, this shift in open probability at positive potentials was completely reversed by the addition of DTT to the VDAC-Cys prior to reconstitution of channels (Fig. 5*B*) as well as after their reconstitution when DTT was added to the membrane-surrounding buffer solution (supplemental Fig. 1 and Table 1). These data, together with the Coomassie Blue gel that shows two bands of VDAC-Cys without Cu-Ph or DTT treatment (Fig. 2), strongly suggest that a significant portion of VDAC-Cys have generated disulfide bonds even before the addition of Cu-Ph. The spontaneous formation of a disulfide bond is reasonable, considering the close proximity of Leu-10 and Ala-170 (Fig. 1*B*). Analogous results have been reported for the bacterial porin, OmpF (35), where a series of Cys mutations were generated between residues in the constriction loop and the wall of the β-barrel in which no alterations in voltage gating were observed upon cross-linking.

There are now a number of lines of evidence that the N terminus does not undergo independent dynamic rearrangements. The first indications of a stable N terminus arose from NMR studies on human VDAC1 by Wagner's group (37). Spectra were collected in the "open" conformations as well as under conditions known to "close" the channel (in the presence of NADH). Although significant spectral shifts were observed, the assignment for the external portion of the N terminus remained the same in both open and closed conformations. A more recent solid state NMR study provided a more complete assignment of human VDAC1, including the N-terminal segment (44). The authors were able to demonstrate that the N-terminal segment stabilizes the integrity of the β-barrel by monitoring major spectral shifts between full-length protein and the N-terminal deletion protein. Supporting these data, Popp *et al.* (45) observed that an N-terminal deletion did not alter VDAC voltage gating but produced noisy channels with a tendency to close, suggesting that the N-terminal region might also be involved in the stabilization of the open state. Finally, the cross-linking data presented here strongly suggest that the α-helix remains inside the channel's pore attached to β-strand 11 when VDAC is open. During voltage-induced gating, the N-terminal region either stays inside the pore or moves in a concerted fashion with the rest of the voltage sensor rather than exerting large independent structural rearrangements to achieve voltage-dependent gating. It should be noted that the data presented here still permit the translocation of the N terminus in and out of the lumen upon gating, as suggested previously (16, 20, 32, 46), as long as this movement is coordinated with the voltage sensor.

If voltage gating does not involve rearrangements of the N-terminal segment, then how is voltage gating achieved? There is still no clear structural understanding of VDAC dynamics, but a new mechanism is emerging; the barrel wall becomes elongated, and the pore narrows around the intact N-terminal segment to exclude nucleotides. Using a combination of NMR, hydrogen/deuterium exchange, and MD simulations, Villinger *et al.* (30) showed pronounced dynamics in β-strands 1–6 and 16–19. The analysis of the *B*-factors from

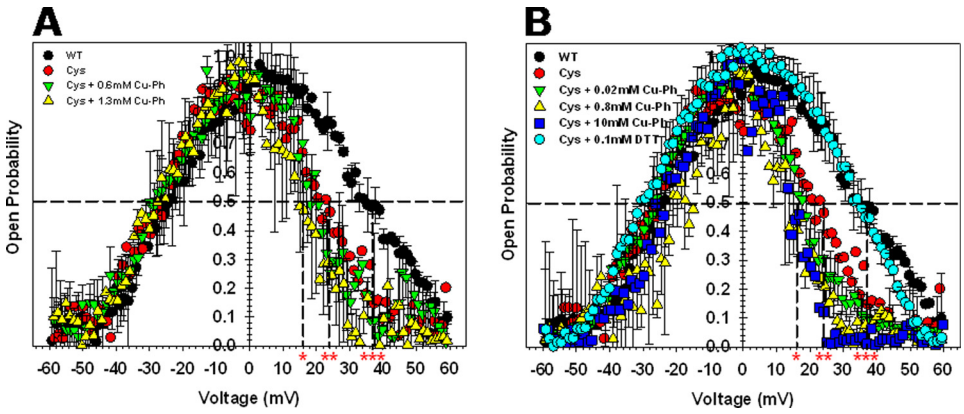

FIGURE 5. **Cross-linking before or after VDAC-Cys reconstitution into the planar membrane does not change channel voltage gating.** *A*, probability to be open or closed at different potentials for VDAC WT, VDAC-Cys, and VDAC-Cys treated with 0.6 or 1.3 mM cross-linker Cu-Ph after channel reconstitution as shown in Fig. 4. The positive potentials at which half of the channels are open and half are closed (V_0) are shown for VDAC WT (***), VDAC-Cys (**), and VDAC-Cys + 1.3 mM Cu-Ph (*). *B*, open probability plots of VDAC1 WT, VDAC-Cys, and VDAC-Cys preincubated with 0.02, 0.8, and 10 mM Cu-Ph or with 0.1 mM DTT in VDAC isolation buffer prior to reconstitution of channels. The positive V_0 values are shown for VDAC WT and VDAC-Cys + 0.1 mM DTT (***), VDAC-Cys (**), and VDAC-Cys + 10 mM Cu-Ph (*). Open probabilities are defined as the ratio $(G - G_{min})/(G_{max} - G_{min})$, where G_{max} and G_{min} are the maximum and minimum conductance, respectively. In each experiment, current records were collected in response to 5–8 periods of triangular voltage waves. Only the part of the wave during which the channels were reopening was used for the subsequent analysis. Data are means of two or three independent experiments ± S.D. (*error bars*). For illustrative clarity, only some of the data display *error bars*.

TABLE 1

Voltage gating parameters, V_0 and *n*, of VDAC WT, VDAC-Cys, and VDAC-Cys treated with different concentrations of Cu-Ph cross-linker after VDAC-Cys reconstitution into planar membrane (in bath) or pretreated with Cu-Ph or DTT in tube prior to channel reconstitution

V_0, the voltage at which half of the channels are open, and *n*, the effective gating charge, were calculated from the open probability plots (Fig. 5) at positive and negative voltages, as described previously (25). Data are means ± S.D., and the number of experiments per condition is indicated in parentheses.

rmVDAC	Positive potentials		Negative potentials	
	V_0	*n*	V_0	*n*
	mV		*mV*	
VDAC WT (2)	37.5 ± 2.4	2.8 ± 0.5	23.8 ± 3.5	2.6 ± 0.2
VDAC-Cys (3)	24.7 ± 4.4	2.4 ± 1.1	25.2 ± 2.8	2.3 ± 0.5
VDAC-Cys + 0.6 mM Cu-Ph (in bath) (2)	19.4 ± 1.9	3.8 ± 1.9	26.6 ± 3.1	2.7 ± 0.2
VDAC-Cys + 1.3 mM Cu-Ph (in bath) (2)	16.7 ± 4.9	2.4 ± 0.5	26.4 ± 4.4	2.9 ± 0.03
VDAC-Cys + 0.8 mM Cu-Ph (in tube) (3)	16.1 ± 2.4	3.8 ± 0.1	20.3 ± 6.2	2.1 ± 2.9
VDAC-Cys + 10 mM Cu-Ph (in tube) (1)	18.5	3.0	23.7	3.2
VDAC-Cys + 0.1 mM DTT (in tube) (2)	36.5 ± 1.1	1.9 ± 0.9	28.3 ± 3.8	2.8 ± 1.1

our original crystal structure supports these data where these same regions have increased *B*-factors (>20%) compared with the β-strand flanking the N-terminal helix (β-strands 8–15), indicating that β-strands 8–15 and the α-helix have a more rigid structure than the remainder of the pore. Also, initial computational attempts to model the voltage dependence of gating through movements in the N-terminal helix alone failed to produce large enough gating charge values (29), hinting at the possibility that the rearrangement is more extensive.

Until recently, β-barrel proteins were considered to be rigid structures due to their vast hydrogen bonding network, but large conformational changes have recently been observed for the outer membrane protein FimD (47). In the apo conformation, this 24-stranded β-barrel protein has an oval shape with a 52 × 28 Å diameter. Upon activation, FimD forms a complex with FimC-FimH, and the pore becomes more circular, with a 44 × 36 Å diameter. It is worth mentioning that the apo form of FimD also has segments of high *B*-factors corresponding to the regions with the largest movements. It is thus tempting to envision a similar mechanism for VDAC where the pore would collapse around the N terminus to achieve closure. Interestingly, it was recently suggested that the conformational transition of VDAC during voltage gating could be sensitive to pressure changes in the hydrocarbon area of the membrane (25), which supports the hypothesis of the soft or flexible part of the VDAC β-barrel. Taking together the current understanding of VDAC structure/function, there is a reasonable probability that the barrel undergoes partial constriction (and possibly simultaneous elongation along the axis perpendicular to the membrane narrowing the pore). Importantly, this does not contradict previous models where part of the β-barrel together with the α-helix move in concert upon gating and slide out of the channel lumen toward the membrane interface (1, 36). The correct model for the transition mechanism between the open and closed conformations of the channel that reconciles all the reliable experimental data will be achieved after further evaluation of the data from molecular dynamics, structural, and biophysical techniques.

Acknowledgments—We thank Sergey Bezrukov, Michael Grabe, Thomas Vondriska, Aviv Paz, and members of the Abramson laboratory for fruitful discussions.

REFERENCES

1. Colombini, M., Blachly-Dyson, E., and Forte, M. (1996) VDAC, a channel in the outer mitochondrial membrane. *Ion Channels* **4,** 169–202
2. Rostovtseva, T. K., Sheldon, K. L., Hassanzadeh, E., Monge, C., Saks, V., Bezrukov, S. M., and Sackett, D. L. (2008) Tubulin binding blocks mito-

chondrial voltage-dependent anion channel and regulates respiration. *Proc. Natl. Acad. Sci. U.S.A.* **105,** 18746–18751
3. Colombini, M. (2004) *Mol. Cell Biochem.* **256**, 107–115
4. Lemasters, J. J., and Holmuhamedov, E. (2006) Voltage-dependent anion channel (VDAC) as mitochondrial governator. Thinking outside the box. *Biochim. Biophys. Acta* **1762,** 181–190
5. Tsujimoto, Y. (2002) *Biosci. Rep.* **22,** 47–58
6. Jacotot, E., Ferri, K. F., El Hamel, C., Brenner, C., Druillennec, S., Hoebeke, J., Rustin, P., Métivier, D., Lenoir, C., Geuskens, M., Vieira, H. L., Loeffler, M., Belzacq, A. S., Briand, J. P., Zamzami, N., Edelman, L., Xie, Z. H., Reed, J. C., Roques, B. P., and Kroemer, G. (2001) Control of mitochondrial membrane permeabilization by adenine nucleotide translocator interacting with HIV-1 viral protein rR and Bcl-2. *J. Exp. Med.* **193,** 509–519
7. Shoshan-Barmatz, V., Keinan, N., Abu-Hamad, S., Tyomkin, D., and Aram, L. (2010) Apoptosis is regulated by the VDAC1 N-terminal region and by VDAC oligomerization. Release of cytochrome *c*, AIF and Smac/Diablo. *Biochim. Biophys. Acta* **1797,** 1281–1291
8. Das, S., Wong, R., Rajapakse, N., Murphy, E., and Steenbergen, C. (2008) Glycogen synthase kinase 3 inhibition slows mitochondrial adenine nucleotide transport and regulates voltage-dependent anion channel phosphorylation. *Circ. Res.* **103,** 983–991
9. Rostovtseva, T., and Colombini, M. (1997) VDAC channels mediate and gate the flow of ATP. Implications for the regulation of mitochondrial function. *Biophys. J.* **72,** 1954–1962
10. Colombini, M. (1989) Voltage gating in the mitochondrial channel, VDAC. *J. Membr. Biol.* **111,** 103–111
11. Gurnev, P. A., Rostovtseva, T. K., and Bezrukov, S. M. (2011) Tubulin-blocked state of VDAC studied by polymer and ATP partitioning. *FEBS Lett.* **585,** 2363–2366
12. Hodge, T., and Colombini, M. (1997) Regulation of metabolite flux through voltage-gating of VADC channels. *J. Membr. Biol.* **157,** 271–279
13. Zimmerberg, J., and Parsegian, V. A. (1986) Polymer inaccessible volume changes during opening and closing of a voltage-dependent ionic channel. *Nature* **323,** 36–39
14. Song, J., Midson, C., Blachly-Dyson, E., Forte, M., and Colombini, M. (1998) The sensor regions of VDAC are translocated from within the membrane to the surface during the gating processes. *Biophys. J.* **74,** 2926–2944
15. Blachly-Dyson, E., Peng, S., Colombini, M., and Forte, M. (1990) Selectivity changes in site-directed mutants of the VDAC ion channel. Structural implications. *Science* **247,** 1233–1236
16. Song, J., Midson, C., Blachly-Dyson, E., Forte, M., and Colombini, M. (1998) The topology of VDAC as probed by biotin modification. *J. Biol. Chem.* **273,** 24406–24413
17. De Pinto, V., Messina, A., Accardi, R., Aiello, R., Guarino, F., Tomasello, M. F., Tommasino, M., Tasco, G., Casadio, R., Benz, R., De Giorgi, F., Ichas, F., Baker, M., and Lawen, A. (2003) New functions of an old protein. The eukaryotic porin or voltage-dependent anion-selective channel (VDAC). *Ital. J. Biochem.* **52,** 17–24
18. De Pinto, V., Reina, S., Guarino, F., and Messina, A. (2008) Structure of the voltage-dependent anion channel. State of the art. *J. Bioenerg. Biomembr.* **40,** 139–147
19. Reymann, S., Florke, H., Heiden, M., Jakob, C., Stadtmuller, U., Steinacker, P., Lalk, V. E., Pardowitz, I., and Thinnes, F. P. (1995) Further evidence of multitopological localization of mammalian protein (VDAC) in the plasmalemma forming part of a chloride channel complex affected in cystic fibrosis and encephalopathy. *Biochem. Mol. Med.* **54,** 75–87
20. Guo, X. W., Smith, P. R., Cognon, B., D'Arcangelis, D., Dolginova, E., and Mannella, C. A. (1995) Molecular design of the voltage-dependent, nion-selective channel in the mitochondrial outer membrane. *J. Struct. Biol.* **114,** 41–59
21. Hiller, S., Garces, R. G., Malia, T. J., Orekhov, V. Y., Colombini, M., and Wagner, G. (2008) Solution structure of the integral human membrane protein VDAC-1 in detergent micelles. *Science* **321,** 1206–1210
22. Bayrhuber, M., Meins, T., Habeck, M., Becker, S., Giller, K., Villinger, S., Vonrhein, C., Griesinger, C., Zweckstetter, M., and Zeth, K. (2008) Structure of the human voltage-dependent anion channel. *Proc. Natl. Acad. Sci. U.S.A.* **105,** 15370–15375
23. Ujwal, R., Cascio, D., Colletier, J. P., Faham, S., Zhang, J., Toro, L., Ping, P., and Abramson, J. (2008) The crystal structure of mouse VDAC1 at 2.3 Å resolution reveals mechanistic insights into metabolite gating. *Proc. Natl. Acad. Sci. U.S.A.* **105,** 17742–17747
24. Kobashi, K. (1968) Catalytic oxidation of sulfhydryl groups by *o*-phenanthroline copper complex. *Biochim. Biophys. Acta* **158,** 239–245
25. Rostovtseva, T. K., Kazemi, N., Weinrich, M., and Bezrukov, S. M. (2006) Voltage gating of VDAC is regulated by nonlamellar lipids of mitochondrial membranes. *J. Biol. Chem.* **281,** 37496–37506
26. Zizi, M., Byrd, C., Boxus, R., and Colombini, M. (1998) The voltage-gating process of the voltage-dependent anion channel is sensitive to ion flow. *Biophys. J.* **75,** 704–713
27. Faham, S., and Bowie, J. U. (2002) Bicelle crystallization. A new method for crystallizing membrane proteins yields a monomeric bacteriorhodopsin structure. *J. Mol. Biol.* **316,** 1–6
28. Ujwal, R., Cascio, D., Chaptal, V., Ping, P., and Abramson, J. (2009) Crystal packing analysis of murine VDAC1 crystals in a lipidic environment reveals novel insights on oligomerization and orientation. *Channels* **3,** 167–170
29. Choudhary, O. P., Ujwal, R., Kowallis, W., Coalson, R., Abramson, J., and Grabe, M. (2010) The electrostatics of VDAC: implications for selectivity and gating. *J. Mol. Biol.* **396,** 580–592
30. Villinger, S., Briones, R., Giller, K., Zachariae, U., Lange, A., de Groot, B. L., Griesinger, C., Becker, S., and Zweckstetter, M. (2010) Functional dynamics in the voltage-dependent anion channel. *Proc. Natl. Acad. Sci. U.S.A.* **107,** 22546–22551
31. Casadio, R., Jacoboni, I., Messina, A., and De Pinto, V. (2002) A 3D model of the voltage-dependent anion channel (VDAC). *FEBS Lett.* **520,** 1–7
32. Mannella, C. A. (1998) Conformational changes in the mitochondrial channel protein, VDAC, and their functional implications. *J. Struct. Biol.* **121,** 207–218
33. Chaptal, V., Ujwal, R., Nie, Y., Watanabe, A., Kwon, S., and Abramson, J. (2010) Fluorescence detection of heavy atom labeling (FD-HAL): a rapid method for identifying covalently modified cysteine residues by phasing atoms. *J. Struct. Biol.* **171,** 82–87
34. Bainbridge, G., Armstrong, G. A., Dover, L. G., Whelan, K. F., and Lakey, J. H. (1998) Displacement of OmpF loop 3 is not required for the membrane translocation of colicins N and A *in vivo*. *FEBS Lett.* **432,** 117–122
35. Bainbridge, G., Mobasheri, H., Armstrong, G. A., Lea, E. J., and Lakey, J. H. (1998) Voltage-gating of *Escherichia coli* porin. A cystine-scanning mutagenesis study of loop 3. *J. Mol. Biol.* **275,** 171–176
36. Colombini, M. (2009) The published 3D structure of the VDAC channel: native or not? *Trends Biochem. Sci.* **34,** 382–389
37. Hiller, S., and Wagner, G. (2009) The role of solution NMR in the structure determinations of VDAC-1 and other membrane proteins. *Curr. Opin. Struct. Biol.* **19,** 396–401
38. Vander Heiden, M. G., Li, X. X., Gottleib, E., Hill, R. B., Thompson, C. B., and Colombini, M. (2001) Bcl-xL promotes the open configuration of the voltage-dependent anion channel and metabolite passage through the outer mitochondrial membrane. *J. Biol. Chem.* **276,** 19414–19419
39. Xu, X., Forbes, J. G., and Colombini, M. (2001) Actin modulates the gating of *Neurospora crassa* VDAC. *J. Membr. Biol.* **180,** 73–81
40. Shimizu, S., Konishi, A., Kodama, T., and Tsujimoto, Y. (2000) BH4 domain of antiapoptotic Bcl-2 family members closes voltage-dependent anion channel and inhibits apoptotic mitochondrial changes and cell death. *Proc. Natl. Acad. Sci. U.S.A.* **97,** 3100–3105
41. Azoulay-Zohar, H., Israelson, A., Abu-Hamad, S., and Shoshan-Barmatz, V. (2004) In self-defence. Hexokinase promotes voltage-dependent anion channel closure and prevents mitochondria-mediated apoptotic cell death. *Biochem. J.* **377,** 347–355
42. Shao, L., Kinnally, K. W., and Mannella, C. A. (1996) Circular dichroism studies of the mitochondrial channel, VDAC, from *Neurospora crassa*. *Biophys. J.* **71,** 778–786
43. Hiller, S., Ibraghimov, I., Wagner, G., and Orekhov, V. Y. (2009) Coupled decomposition of four-dimensional NOESY spectra. *J. Am. Chem. Soc.* **131,** 12970–12978
44. Schneider, R., Etzkorn, M., Giller, K., Daebel, V., Eisfeld, J., Zweckstetter, M., Griesinger, C., Becker, S., and Lange, A. (2010) The native conforma-

tion of the human VDAC1 N terminus. *Angew. Chem. Int. Ed. Engl.* **49,** 1882–1885

45. Popp, B., Court, D. A., Benz, R., Neupert, W., and Lill, R. (1996) The role of the N and C termini of recombinant *Neurospora* mitochondrial porin in channel formation and voltage-dependent gating. *J. Biol. Chem.* **271,** 13593–13599
46. Stanley, S., Dias, J. A., D'Arcangelis, D., and Mannella, C. A. (1995) Peptide-specific antibodies as probes of the topography of the voltage-gated channel in the mitochondrial outer membrane of *Neurospora crassa*. *J. Biol. Chem.* **270,** 16694–16700
47. Phan, G., Remaut, H., Wang, T., Allen, W. J., Pirker, K. F., Lebedev, A., Henderson, N. S., Geibel, S., Volkan, E., Yan, J., Kunze, M. B., Pinkner, J. S., Ford, B., Kay, C. W., Li, H., Hultgren, S. J., Thanassi, D. G., and Waksman, G. (2011) Crystal structure of the FimD usher bound to its cognate FimC-FimH substrate. *Nature* **474,** 49–53
48. Gruswitz, F., and Ho, B. K. (2008) HOLLOW: generating accurate representations of channel and interior surfaces in molecular structures. *BMC Struct. Biol.* **8,** 49